PCCP

PAPER

View Article Online
View Journal | View Issue

Cite this: *Phys. Chem. Chem. Phys.*, 2024, **26**, 463

A minimal kinetic model for the interpretation of complex catalysis in single enzyme molecules

Prasanta Kundu, [a] Soma Saha *[b] and Gautam Gangopadhyay [a]

Received 15th April 2023,
Accepted 15th November 2023

DOI: 10.1039/d3cp01720f

rsc.li/pccp

Multi-exponential waiting-time distribution and randomness parameter greater than unity ascribe dynamic disorder in single-enzyme catalysis corroborated to the interplay of transforming conformers [English *et al.*, *Nat. Chem. Biol.*, 2006, **2**, 87]. The associated multi-state model of enzymatic turnovers with statically heterogeneous catalytic rates misdescribes the non-linear uprising of the randomness parameter from unity in relation to the attributes of the fall-offs of the waiting-time distribution at different substrate concentrations. To resolve this crucial issue, we first employ a comprehensive stochastic reaction scenario and further rationalize and work out the minimal indispensable dynamic-disorder model that ensures the foregoing relationship upon comparison with the data. We elucidate that specific disregard for the transition rate coefficients in the multi-state model on account of the especially slow conformational transitions is the underlying reason for not achieving interrelation between the observables.

1 Introduction

The advent of single-molecule spectroscopy since the last decades has unveiled the role of incessant structural variations of the enzyme molecules in real-time experiments and thereby illustrated the dynamic behaviour of the catalytic rate constant beyond the conventional Michaelis–Menten (MM) kinetics.[1–6] Here, we are acquainted with one such renowned single-molecule fluorescence assay that exposed noteworthy outcomes while the fluorogenic product resorufin is formed from the hydrolysis of resorufin-β-D-galactopyranoside, catalysed by single β-galactosidase enzymes.[7] The lengths of the time that elapsed for each enzymatic turnover, the waiting times, were monitored. Importantly, the prevalence of molecular memory at high substrate concentrations was quite evident and its longevity over the decades featured the interplay between the transforming conformers.

The overview of the experimental outcomes is comprised of the following. Statistical distribution of the waiting times, $f(t)$, executed apparent non-exponentiality at higher substrate concentrations. This fact is indeed inscrutable by the classical kinetics. However, the same attribute of ensemble-level mono-exponentiality in the regime of lower substrate concentration was conserved. Regardless, the kinetics at the ensemble level and the single-molecule level became compatible which was evident from the similar hyperbolic variations of the mean waiting times, $\langle t \rangle$, with the inverse of substrate concentration, represented in accordance with the Lineweaver–Burke fashion.[8] Finally, the randomness parameter, R, the dimensionless variance of the turnover time fluctuations, exhibited a non-linear growth from its initial magnitude of unity with the rising substrate concentration.

The single-β-galactosidase experiment tangibly validated dynamic disorder in the reaction pathway when the substrate concentrations are large. This point along with the hyperbolic variation of $\langle t \rangle$ and the change of R from unity at low [S] to $R > 1$ at high [S] were qualitatively demonstrated by prior analysis of the Michaelis–Menten kinetics at the single-molecule level. The proposed model considered multiple conformational substates of the enzyme and the enzyme–substrate complex and was governed by the condition of quasi-static limit associated with much slower conformational transitions as compared to the catalytic rate.[9] The authors estimated the overall waiting-time distribution by obtaining the steady-state weighted averages of the distribution corresponding to the reaction channel of every conformer. Simplification of the calculated results was achieved by assigning certain assumptions and retaining dynamic disorder exclusively in the catalytic step. Later, the same approximate model was employed unaltered to recover the outcomes of the time-dependent decay of $f(t)$ and the linear increment of $\langle t \rangle$ with growing $\frac{1}{[S]}$ quantitatively.[7] In contrast, no comparison was made with the observed data for the randomness parameter.

In successive studies it was discerned that the multi-state tool remained unable to show the differences between the magnitudes of R at altered substrate concentrations.[10,11] A constant quantity of R contradicts straightaway the observed variations of the waiting-time distribution towards higher

[a] *S. N. Bose National Centre for Basic Sciences, Block JD, Sector III, Salt Lake, Kolkata 700106, India*
[b] *Department of Chemistry, Presidency University, 86/1 College Street, Kolkata 700073, India. E-mail: soma.chem@presiuniv.ac.in*

substrate concentration. Hence, the formulation of the multi-state reaction model led to the incompatible qualitative and quantitative predictions of the dependence of R on the substrate concentration and stayed away from a foolproof explanation of the experimental set of data.

It is known that simpler models[12] of dynamic disorder are usable to explain the histograms of the reaction times and the corresponding mean values acceptably well.[11] More instances are discussed in recent works where heterogeneous kinetics from the distinct single-molecule studies[13–20] were rationalized with the aid of two-state[21–23] and the multi-state[24] frameworks. The better suitability of a proposed single-molecule kinetic model can be realized with reference to the higher moments of the statistical distribution. In the kinetic measurements of single β-galactosidase catalysis, the randomness parameter is the sole quantity described using the second moment of the waiting-time distribution.[9] As a result, it is desirable that further regard to a kinetic framework for the given single-enzyme reaction will regenerate the observed time-distributions and the quantified randomness, described by the magnitudes of R, besides satisfying the mean values of the distribution function.

An earlier work[10] considered the non-Poisson renewal reaction processes for single catalytic turnover in which the basic idea was to represent the turnover time distribution in terms of the three reaction time distributions of the elementary reversible and irreversible reaction processes.[25] Subsequently, an excellent quantitative illustration of the behaviour of the parameter R was provided. Specifically, to the best of our knowledge, no emphatic model of stochastic chemical kinetics is available to date that rendered unified quantitative interpretation of the waiting-time distribution data and the randomness parameter data over the full range of chosen substrate concentration. It is indeed quite profound to possess this idea since it would direct a way out of the conflict caused by the exploitation of the same multi-state theory from the qualitative and quantitative perspectives.

To resolve the issue, a dynamic probe[11] was proposed meanwhile that was shaped by the aspects of dynamical disorder in the line of Zwanzig's conception[26] and the dynamics of a flexible polymer.[27,28] This very model appeared successful to provide satisfactory explanations for the entire set of experimental data. The model however was unrelated with the conventional stepwise chemical conversions and structural dynamics of the active species was the principal trait of prolonged calculations. Nevertheless, remarkably, a worthy justification of dimensional analysis for a key model parameter accomplished immediate comparison with the data. To this end, we note that, in ref. 9, no use of the primary two-state model of dynamic disorder was made to check the qualitative tendencies of the measurable stochastic kinetic parameters. On the other hand, ref. 11 demonstrated that an application of the two-state kinetic scheme, involving product formation through either the single or parallel catalytic paths, best matched the numerals of R at the regime of low substrate concentration, in addition to satisfying the measured histograms and mean times for product formation. A concern for the whole scenario therefore motivated us to recognise the minimal kinetic model around the central theme

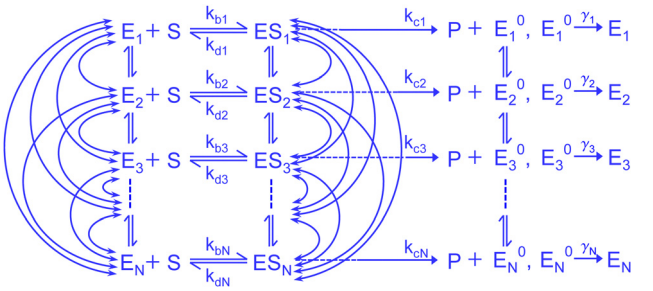

Fig. 1 Comprehensive kinetic scheme of the Michaelis–Menten mechanism consisting of large finite interconverting conformers of the active species. The parallel transitions $E_i^0 \leftrightarrow E_j^0$ and the rate constants, namely, λ_{ij}, λ_{ji}, ε_{ij}, ε_{ji} and ζ_{ij}, ζ_{ji}, that characterize the $E_i \leftrightarrow E_j$, $ES_i \leftrightarrow ES_j$ and $E_i^0 \leftrightarrow E_j^0$ transitions, respectively are not shown for simplicity.

of affirming the surpass of R from unity in consonance with the changing exponentiality of the waiting-time distribution.

In the present work, we consider a comprehensive kinetic framework of single-enzyme catalysis in which the duplex states of the enzyme, E and ES, interconvert among finite number (N) of conformational substates. We show the mesh of transition paths such that any active isomer X_i (X stands for E, ES and E^0) is allowed to make transitions to the $N-1$ numbers of X_j across vertically (Fig. 1). It is alike with the multi-state model suggested by Kou *et al.*[9] who acknowledged the multitude of transition possibilities while extending the methodology applied to the two-conformer case. The notable outlook of their analysis involved insertion of limiting conditions to depict the relevance of the ensemble Michaelis–Menten kinetics in the presence of structural dynamics of the enzyme molecule. Several convenient assumptions finally resulted in a fairly simple expression for the waiting-time distribution. The latter was defined by the integration of the product of the waiting-time distribution for the single reaction channel (in the absence of dynamic disorder) and the specific distribution complied with by the catalytic rate constant. Since this average distribution apposite to statically heterogeneous enzymatic description led to significant discrepancy with the available randomness data, the importance of the explicit subsistence of the transition coefficients within the calculated results needs to be assessed. Thereupon, it may be attempted to revisit the analysis making it free from the previous suppositions. Furthermore, despite the fact that the multiplicity of states for a real enzyme is soundly factual, a straightforward analytical evaluation of the reaction time distribution and other parameters of interest, retaining large finite number of substates and waiving the working approximations, would become utterly complex. Consequently, it seems quite methodic to abridge the multi-channel kinetic framework to one having a lower finite integer of conformers. This minimal model, in turn, ought to be enlarged compared with the two-state layout for which a worthy comparison of the theoretical results with the data would finally substantiate the effectiveness of the given model description.

The arrangement of the paper includes a description of the state-based model in Section 2. A comparison of the predicted results with the measured data is presented in Section 3. Finally, we present our conclusions in Section 4.

2 Kinetic model

Enzyme-catalyzed reactions when considered at the single-molecule level represent stochastic events.[29–31] A kinetic reinvestigation is made here to fulfill our aim to interpret fully the characteristic relationship between the waiting-time distribution and the randomness parameter.

Fig. 1 represents a comprehensive stochastic kinetic scheme of catalysis by a fluctuating single enzyme molecule. We take into consideration all possible transitions among the pairs of conformers and the parallel paths of product formation from every substate of the enzyme–substrate complex. To start with, the time evolution of the probability of the various possible states can be expressed as follows (we use the symbol P for probability throughout the calculations).[32]

$$\dot{P}_{\mathrm{E}_i}(t) = -\left(k_{\mathrm{b}i}[\mathrm{S}] + \sum_{j=1,\, j\neq i}^{N} \lambda_{ij}\right) P_{\mathrm{E}_i}(t) + k_{\mathrm{d}i} P_{\mathrm{ES}_i}(t) + \sum_{j=1,\, j\neq i}^{N} \lambda_{ji} P_{\mathrm{E}_j}(t) \tag{1}$$

$$\dot{P}_{\mathrm{ES}_i}(t) = k_{\mathrm{b}i}[\mathrm{S}] P_{\mathrm{E}_i}(t) - \left(k_{\mathrm{d}i} + k_{\mathrm{c}i} + \sum_{j=1,\, j\neq i}^{N} \varepsilon_{ij}\right) P_{\mathrm{ES}_i}(t) + \sum_{j=1,\, j\neq i}^{N} \varepsilon_{ji} P_{\mathrm{ES}_j}(t) \tag{2}$$

$$\dot{P}_{\mathrm{E}_i^0}(t) = k_{\mathrm{c}i} P_{\mathrm{ES}_i}(t) \tag{3}$$

The indexes i and j vary from 1 to N. $k_{\mathrm{b}i}$, $k_{\mathrm{d}i}$ and $k_{\mathrm{c}i}$ represent the rate constants for the binding of the substrate with the i-th conformer of the enzyme to form the ES_i complex, unbinding rate constants and the catalytic rate constants, respectively. The structural transitions between the i-th and j-th conformers of the enzyme and enzyme–substrate complex are governed by λ_{ij}, λ_{ji} and ε_{ij}, ε_{ji}. $\mathrm{E}_i^0 \rightarrow \mathrm{E}_i$ transitions are assumed instantaneous and hence ζ_{ij}, ζ_{ji} and γ_i are not involved in the rate equations.

It is to be noted that Fig. 1 depicts a generalized kinetic scheme and it may be desirable to opt for suitable assumption and approximation that would simplify the mathematical treatment. However, any such assumption or approximation should leave the portray of the reaction network unmodified. Referring to the parent work of Kou *et al.*, it is assumed that the energy barrier between the two minima on the free-energy surface associated with E_i^0 and E_i is negligible and hence the approximation $\gamma_i \rightarrow \infty$ is rational. Moreover, for the case of $\mathrm{E}_i^0 \leftrightarrow \mathrm{E}_j^0$ conversions, the same assumption is followed and ζ_{ij}, $\zeta_{ji} \rightarrow \infty$ ($\mathrm{E}_i^0 \rightarrow \mathrm{E}_i$ and $\mathrm{E}_i^0 \leftrightarrow \mathrm{E}_j^0$ transitions occur after the product formation). Consequently, these rate constants do not appear in the governing kinetic equations. Eqn (1)–(3) must fulfill the constraint $\sum_{i=1}^{N}\left(P_{\mathrm{E}_i}(t) + P_{\mathrm{ES}_i}(t) + P_{\mathrm{E}_i^0}(t)\right) = 1$ at any time t with the specified initial conditions of $P_{\mathrm{E}_1}(0) = 1$, $P_{\mathrm{E}_{i\neq 1}}(0) = 0$, $P_{\mathrm{ES}_i}(0) = 0$, and $P_{\mathrm{E}_i^0}(0) = 0$.

The formation of the fluorogenic product resorufin traced the completion of a single catalytic turnover complemented by the regeneration of the enzyme molecule *via* E_i^0. The time on which the product is formed is familiar as the turnover time or waiting time. Repeated measurements of the enzymatic turnovers yield different waiting times and hence a distribution due to the structural heterogeneity of the enzyme molecule during the course of the reaction. For the single enzymatic reaction, the primary attention is drawn to the waiting-time distribution, $f(t)$. Since in the time interval t and $t + \Delta t$, the probability of an enzymatic turnover occurring, $f(t)\Delta t$, becomes equal to the probability that the enzyme exits in the E_i^0 state, $\Delta P_{\mathrm{E}_i^0}(t)$, then in the limit of $\Delta t \rightarrow 0$, and $f(t)$ is expressed by[9]

$$f(t) = \sum_i \dot{P}_{\mathrm{E}_i^0}(t) = \sum_i k_{\mathrm{c}i} P_{\mathrm{ES}_i}(t) \tag{4}$$

Next, it is crucial to evaluate $f(t)$ from the solutions of the coupled differential equations containing both $P_{\mathrm{E}_i}(t)$ and $P_{\mathrm{ES}_i}(t)$. Prior to that, eqn (1) and (2) are expressed as a set of $2N$ linear differential equations, noted as

$$\frac{\mathrm{d}}{\mathrm{d}t}\mathbf{P} = \mathbf{M}\mathbf{P} \tag{5}$$

where, $\mathbf{P} = [P_{\mathrm{E}_1}(t), \ldots, P_{\mathrm{E}_N}(t), P_{\mathrm{ES}_1}(t), \ldots, P_{\mathrm{ES}_N}(t)]^T$ and

$$\mathbf{M} = \begin{pmatrix} -\left(k_{\mathrm{b}1}[\mathrm{S}] + \sum_{j=2}^{N}\lambda_{1j}\right) & \lambda_{21} & \cdots & \lambda_{N1} & k_{\mathrm{d}1} & 0 & \cdots & 0 \\ \lambda_{12} & -\left(k_{\mathrm{b}2}[\mathrm{S}] + \sum_{j=1,j\neq 2}^{N}\lambda_{2j}\right) & \cdots & \lambda_{N2} & 0 & k_{\mathrm{d}2} & \cdots & 0 \\ \vdots & \vdots & \ddots & \vdots & \vdots & \vdots & \ddots & \vdots \\ \lambda_{1N} & \lambda_{2N} & \cdots & -\left(k_{\mathrm{b}N}[\mathrm{S}] + \sum_{j=1}^{N-1}\lambda_{Nj}\right) & 0 & 0 & \cdots & k_{\mathrm{d}N} \\ k_{\mathrm{b}1}[\mathrm{S}] & 0 & \cdots & 0 & -\left(k_{\mathrm{c}1} + k_{\mathrm{d}1} + \sum_{j=2}^{N}\varepsilon_{1j}\right) & \varepsilon_{21} & \cdots & \varepsilon_{N1} \\ 0 & k_{\mathrm{b}2}[\mathrm{S}] & \cdots & 0 & \varepsilon_{12} & -\left(k_{\mathrm{c}2} + k_{\mathrm{d}2} + \sum_{j=1,j\neq 2}^{N}\varepsilon_{2j}\right) & \cdots & \varepsilon_{N2} \\ \vdots & \vdots & \ddots & \vdots & \vdots & \vdots & \ddots & \vdots \\ 0 & 0 & \cdots & k_{\mathrm{b}N}[\mathrm{S}] & \varepsilon_{1N} & \varepsilon_{2N} & \cdots & -\left(k_{\mathrm{c}N} + k_{\mathrm{d}N} + \sum_{j=1}^{N-1}\varepsilon_{Nj}\right) \end{pmatrix} \tag{6}$$

It is likely to be mentioned here that the $2N \times 2N$ matrix $\mathbf{M}$ can be block-factorized into four $N \times N$ matrices producing[9]

$$\mathbf{M} = \begin{pmatrix} \mathbf{M}_{X_{\text{in}}} - \mathbf{M}_{XY} - \mathbf{M}_{X_{\text{out}}} & \mathbf{M}_{YX} \\ \mathbf{M}_{XY} & \mathbf{M}_{Y_{\text{in}}} - \mathbf{M}_{YX} - \mathbf{M}_{YZ} - \mathbf{M}_{Y_{\text{out}}} \end{pmatrix} \tag{7}$$

in which the subscripts X, Y and Z represent the states E, ES and E^0, respectively. We describe the structures of the seven individual terms that construct eqn (7) upon different combinations in Appendix A.

The initial conditions rational to eqn (5) are given by $\mathbf{P}_0 = [1, 0, \ldots, 0, \ldots, 0]^T$. Eqn (5), upon Laplace transform, an integral transformation defined by[33]

$$\mathscr{L}\{g(t)\} = G(s) = \int_0^\infty \mathrm{e}^{-st} g(t)\mathrm{d}t, \tag{8}$$

followed by the imposition of the initial conditions, yields the Laplace space solutions of eqn (1) and (2), which may be expressed as

$$\mathbf{P}(s) = [s\mathbf{I} - \mathbf{M}]^{-1}\mathbf{P}_0 \tag{9}$$

where $\mathbf{I}$ is the unit matrix.

To evaluate $f(t)$, one needs to invert the Laplace-transformed solutions $\mathbf{P}(s)$, given in the preceding equation. Once known, $f(t)$ leads to the generation of the various moments, formulated as[34]

$$\langle t^v \rangle = \int_0^\infty t^v f(t)\mathrm{d}t, \tag{10}$$

with $v = 1,2,\ldots$ that are apt for describing the other parameters of experimental interest. Namely, the first moment exhibits the mean waiting time, whilst the randomness parameter is narrated as the ratio of variance to the square of the mean waiting time,

$$R = \frac{\langle t^2 \rangle - \langle t \rangle^2}{\langle t \rangle^2} \tag{11}$$

An alternate manner to compute the moments is accomplished from

$$\langle t^v \rangle = (-1)^v \frac{\mathrm{d}^v F(s)}{\mathrm{d}s^v}\bigg|_{s\to 0} \tag{12}$$

where $F(s)$ is the Laplace transform of $f(t)$.

We have introduced all the prerequisites to proceed further in our analysis. At this point, however, we ponder the following fact. The essence of structural variations of the active species, enzyme and enzyme–substrate complex, that was earlier depicted with the two-state model came out efficient to elucidate the randomness parameter data at substrate concentrations not exceeding 20 μM. Beyond the latter, the steady growth of predicted R continued with the lower estimates than the data, as opposed to the constancy of results achieved by the multi-state model.[11] Hence, a kinetic design is required which should be more extensive than the two-conformer description and unfollowed by the particularities of the conditions and assumptions of the multi-state model[9] as well. Apparently, a set of kinetic schemes can be thought of that become distinct with regard to the number of reaction paths. It is customary to derive expressions for the observables related to every kinetic scheme, *i.e.* one needs to assign specific numbers of conformers of the active species in the comprehensive sketch (Fig. 1). Larger than a two-state model, any given scheme accounts for a greater number of mutual transitions among the conformational isomers that better befit the dynamic disorder scenario. However, switching to a higher state description imparts intensive complexity in analytical calculations, unaccompanied with working approximations, and gives rise to a significant increase in the number of adjustable parameters that need to be fixed suitably. Therefore, we reason that our primary choice concerns the three-conformer parallel pathway model to continue the illustration.

Consider the threefold coupled reaction description of the single-enzyme kinetics, shown in Fig. 2. It is characterized by nine reaction rate constants and twelve transition coefficients. In contrast to the two-conformer analogue,[11,12] it offers the simplest model in which multitudes of conformational transitions for a given isomer is realized. Setting $N = 3$ in eqn (1) and (2), we arrive at the following revised forms of the involved matrices.

$$\mathbf{P}(s) = [P_{\mathrm{E}_1}(s), P_{\mathrm{E}_2}(s), P_{\mathrm{E}_3}(s), P_{\mathrm{ES}_1}(s), P_{\mathrm{ES}_2}(s), P_{\mathrm{ES}_3}(s)]^T \tag{13}$$

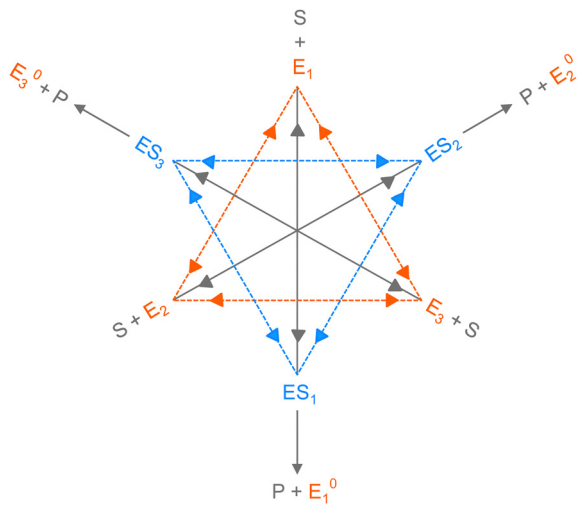

Fig. 2 The three-conformer kinetic model of single-enzyme catalysis. Reversible transitions between the conformers of the enzyme and the conformers of the enzyme–substrate complex are shown by the sides of the orange and blue triangles, respectively. The rate constants for $E_i \leftrightarrow E_j$ and $ES_i \leftrightarrow ES_j$ conversions are specified by λ_{ij}, λ_{ji} and ε_{ij}, ε_{ji}, respectively, where i and j range from 1–3 and $j \neq i$. The long gray reversible arrows indicate the substrate binding with E_i and the dissociation of ES_i, governed by k_{bi} and k_{di}, respectively. The parallel paths of product formation from different ES_i are depicted by short gray arrows with the rate constants k_{ci}. $E_i^0 \rightarrow E_j^0$ and $E_i^0 \rightarrow E_i$ transitions are not shown here.

with $\mathbf{P}_0 = [1,0,0,0,0,0]^T$ being the initial condition and

$$s\mathbf{I}-\mathbf{M}=\begin{pmatrix} s+(k_{b1}[S]+\lambda_{12}+\lambda_{13}) & -\lambda_{21} & -\lambda_{31} & -k_{d1} & 0 & 0 \\ -\lambda_{12} & s+(k_{b2}[S]+\lambda_{21}+\lambda_{23}) & -\lambda_{32} & 0 & -k_{d2} & 0 \\ -\lambda_{13} & -\lambda_{23} & s+(k_{b3}[S]+\lambda_{31}+\lambda_{32}) & 0 & 0 & -k_{d3} \\ -k_{b1}[S] & 0 & 0 & s+(k_{c1}+k_{d1}+\varepsilon_{12}+\varepsilon_{13}) & -\varepsilon_{21} & -\varepsilon_{31} \\ 0 & -k_{b2}[S] & 0 & -\varepsilon_{12} & s+(k_{c2}+k_{d2}+\varepsilon_{21}+\varepsilon_{23}) & -\varepsilon_{32} \\ 0 & 0 & -k_{b3}[S] & -\varepsilon_{13} & -\varepsilon_{23} & -(k_{c3}+k_{d3}+\varepsilon_{31}+\varepsilon_{32}) \end{pmatrix} \tag{14}$$

Performing matrix inversion followed by matrix multiplication, one can obtain the elements of $\mathbf{P}(s)$ according to eqn (9). Similar to eqn (7), the inverse of eqn (14) is first expressed as

$$[s\mathbf{I}-\mathbf{M}]^{-1}=\begin{pmatrix} s-\left(\mathbf{M}_{X_{in}}-\mathbf{M}_{XY}-\mathbf{M}_{X_{out}}\right) & -\mathbf{M}_{YX} \\ -\mathbf{M}_{XY} & s-\left(\mathbf{M}_{Y_{in}}-\mathbf{M}_{YX}-\mathbf{M}_{YZ}-\mathbf{M}_{Y_{out}}\right) \end{pmatrix}^{-1}_{6\times6} \tag{15}$$

If short notations of the above four 3 × 3 block matrices are coined such that $\mathbf{G} = s - (\mathbf{M}_{X_{in}} - \mathbf{M}_{XY} - \mathbf{M}_{X_{out}})$, $\mathbf{H} = -\mathbf{M}_{YX}$, $\mathbf{W} = -\mathbf{M}_{XY}$ and $\mathbf{Z} = s - (\mathbf{M}_{Y_{in}} - \mathbf{M}_{YX} - \mathbf{M}_{YZ} - \mathbf{M}_{Y_{out}})$, then eqn (15) is further constructed by the method of block matrix inversion, producing

$$[s\mathbf{I}-\mathbf{M}]^{-1}=\begin{pmatrix} (\mathbf{G}-\mathbf{H}\mathbf{Z}^{-1}\mathbf{W})^{-1} & -(\mathbf{G}-\mathbf{H}\mathbf{Z}^{-1}\mathbf{W})^{-1}\mathbf{H}\mathbf{Z}^{-1} \\ -\mathbf{Z}^{-1}\mathbf{W}(\mathbf{G}-\mathbf{H}\mathbf{Z}^{-1}\mathbf{W})^{-1} & (\mathbf{Z}-\mathbf{W}\mathbf{G}^{-1}\mathbf{H})^{-1} \end{pmatrix}_{6\times6} \tag{16}$$

One important aspect of the solution is to be noticed during matrix multiplication. Every element of $\mathbf{P}_0$ is zero except the first one. Since the vector $\mathbf{P}_0$ multiplies $[s\mathbf{I} - \mathbf{M}]^{-1}$, therefore, the first column of $[s\mathbf{I} - \mathbf{M}]^{-1}$ will contribute exclusively to the multiplication output.[35] The first three rows of the latter correspond to the probabilities of three conformers of the specie E, while its last three rows yield the probabilities of ES conformers in the Laplace domain. Because the definition of waiting-time distribution, eqn (3), involves the $P_{ES_i}(t)$ terms, it is evident that the first column of the block matrix, $-\mathbf{Z}^{-1}\mathbf{W}(\mathbf{G} - \mathbf{H}\mathbf{Z}^{-1}\mathbf{W})^{-1}$ in eqn (16) will be our only concern. Subsequently, the abbreviated expressions for $P_{ES_1}(s)$, $P_{ES_2}(s)$ and $P_{ES_3}(s)$ are obtained which show that

$$P_{ES_1}(s) = \frac{\eta_{14}s^4 + \eta_{13}s^3 + \eta_{12}s^2 + \eta_{11}s + \eta_{10}}{s^6 + \delta_5 s^5 + \delta_4 s^4 + \delta_3 s^3 + \delta_2 s^2 + \delta_1 s + \delta_0} \tag{17}$$

$$P_{ES_2}(s) = \frac{\eta_{23}s^3 + \eta_{22}s^2 + \eta_{21}s + \eta_{20}}{s^6 + \delta_5 s^5 + \delta_4 s^4 + \delta_3 s^3 + \delta_2 s^2 + \delta_1 s + \delta_0} \tag{18}$$

$$P_{ES_3}(s) = \frac{\eta_{33}s^3 + \eta_{32}s^2 + \eta_{31}s + \eta_{30}}{s^6 + \delta_5 s^5 + \delta_4 s^4 + \delta_3 s^3 + \delta_2 s^2 + \delta_1 s + \delta_0} \tag{19}$$

In eqn (17)–(19), the various η and δ terms that appear in the numerators and the denominators represent the combinatory rate parameters, the explicit forms of which are quite lengthy, except the coefficient of s^4 in eqn (17), and therefore are shown in Appendix B.

The inverse Laplace transforms of eqn (17) is given by

$$\begin{aligned} P_{ES_1}(t) = {} & \frac{(-\eta_{14}r_1^4 + \eta_{13}r_1^3 - \eta_{12}r_1^2 + \eta_{11}r_1 - \eta_{10})}{(r_1-r_2)(r_1-r_3)(r_1-r_4)(r_1-r_5)(r_1-r_6)}e^{-r_1 t} \\ & + \frac{(-\eta_{14}r_2^4 + \eta_{13}r_2^3 - \eta_{12}r_2^2 + \eta_{11}r_2 - \eta_{10})}{(r_2-r_1)(r_2-r_3)(r_2-r_4)(r_2-r_5)(r_2-r_6)}e^{-r_2 t} \\ & + \frac{(-\eta_{14}r_3^4 + \eta_{13}r_3^3 - \eta_{12}r_3^2 + \eta_{11}r_3 - \eta_{10})}{(r_3-r_1)(r_3-r_2)(r_3-r_4)(r_3-r_5)(r_3-r_6)}e^{-r_3 t} \\ & + \frac{(-\eta_{14}r_4^4 + \eta_{13}r_4^3 - \eta_{12}r_4^2 + \eta_{11}r_4 - \eta_{10})}{(r_4-r_1)(r_4-r_2)(r_4-r_3)(r_4-r_5)(r_4-r_6)}e^{-r_4 t} \\ & + \frac{(-\eta_{14}r_5^4 + \eta_{13}r_5^3 - \eta_{12}r_5^2 + \eta_{11}r_5 - \eta_{10})}{(r_5-r_1)(r_5-r_2)(r_5-r_3)(r_5-r_4)(r_5-r_6)}e^{-r_5 t} \\ & + \frac{(-\eta_{14}r_6^4 + \eta_{13}r_6^3 - \eta_{12}r_6^2 + \eta_{11}r_6 - \eta_{10})}{(r_6-r_1)(r_6-r_2)(r_6-r_3)(r_6-r_4)(r_6-r_5)}e^{-r_6 t} \end{aligned} \tag{20}$$

which is conveniently expressed as

$$P_{ES_1}(t) = \sum_{\theta=1}^{6} \frac{-\eta_{14}r_\theta^4 + \eta_{13}r_\theta^3 - \eta_{12}r_\theta^2 + \eta_{11}r_\theta - \eta_{10}}{\prod_{\phi=1,\phi\neq\theta}^{6}(r_\theta - r_\phi)}e^{-r_\theta t} \tag{21}$$

where r_θ and r_ϕ are the effective rate constants, related to the roots of the equation $s^6 + \delta_5 s^5 + \delta_4 s^4 + \delta_3 s^3 + \delta_2 s^2 + \delta_1 s + \delta_0 = 0$.[32] Likewise, $P_{ES_2}(t)$ and $P_{ES_3}(t)$ are also written concisely in the following forms.

$$P_{ES_2}(t) = \sum_{\theta=1}^{6} \frac{\eta_{23}r_\theta^3 - \eta_{22}r_\theta^2 + \eta_{21}r_\theta - \eta_{20}}{\prod_{\phi=1,\phi\neq\theta}^{6}(r_\theta - r_\phi)}e^{-r_\theta t} \tag{22}$$

$$P_{ES_3}(t) = \sum_{\theta=1}^{6} \frac{\eta_{33}r_\theta^3 - \eta_{32}r_\theta^2 + \eta_{31}r_\theta - \eta_{30}}{\prod_{\phi=1,\phi\neq\theta}^{6}(r_\theta - r_\phi)}e^{-r_\theta t} \tag{23}$$

Substituting eqn (21)–(23) into eqn (4), the waiting-time distribution of the three-state stochastic kinetic model is attained, written below.

$$f(t) = \sum_{\theta=1}^{6} \frac{\zeta e^{-r_\theta t}}{\prod_{\phi=1,\phi\neq\theta}^{6} (r_\theta - r_\phi)} \tag{24}$$

where

$$\begin{aligned}\zeta = {} & \left[k_{c1}\left(-\eta_{14} r_\theta^4 + \eta_{13} r_\theta^3 - \eta_{12} r_\theta^2 + \eta_{11} r_\theta - \eta_{10}\right)\right. \\ & + k_{c2}\left(\eta_{23} r_\theta^3 - \eta_{22} r_\theta^2 + \eta_{21} r_\theta - \eta_{20}\right) \\ & \left. + k_{c3}\left(\eta_{33} r_\theta^3 - \eta_{32} r_\theta^2 + \eta_{31} r_\theta - \eta_{30}\right)\right]\end{aligned}$$

Afterwards, evaluations of the first and second moments of $f(t)$ are carried out by making use of eqn (12) and found to be as shown below.

$$\langle t \rangle = \sum_{\theta=1}^{6} \frac{\zeta}{\prod_{\phi=1,\phi\neq\theta}^{6} r_\theta^2 (r_\theta - r_\phi)} \tag{25}$$

$$\langle t^2 \rangle = \sum_{\theta=1}^{6} \frac{2\zeta}{\prod_{\phi=1,\phi\neq\theta}^{6} r_\theta^3 (r_\theta - r_\phi)} \tag{26}$$

Eqn (25) and (26), in turn, provide the randomness parameter from its definition. The numeral of R while exceeding unity manifests that the system under investigation is dynamically disordered.[36]

3 Results and discussions

In this section, we explore whether the exploitation of the key expressions, eqn (24)–(26), would lead to the productive comparison with the data. To execute it, in Fig. 3, we first show the temporal decay profiles of the waiting-time distribution obtained by using eqn (24) (solid lines) with the experimental estimates (symbols) at four substrate concentrations.[7] We observe that our calculated results are in excellent agreement with the measured yields. The variation of the mean waiting times with the progress of inverse of substrate concentration is depicted in Fig. 4a. The theoretical output is the solid line, eqn (25), that efficiently recovers the mean times for product formation (circles). Finally, in Fig. 4b, we turn to look for the resemblance between our predicted randomness (curve) and the reported magnitudes of R (symbols) which is the key concern of our work. The variation of the estimated result upon increasing substrate concentration and the respective similarity with the data are quite remarkable. The adjustable parameters used for fitting in Fig. 3 and 4 are listed in the caption of the former. Therefore, the three-state model successfully restores the characteristic relationship uniting the nature of the decay profiles of the waiting-time distribution to the non-linear variation of the randomness parameter across the experimental range of substrate concentration. If otherwise stated, the present kinetic framework is able to overcome the limitations of the previous kinetic paradigms[7,11,12] and serves as the minimum indispensable model to interpret the outcomes of the single β-galactosidase catalysis altogether.

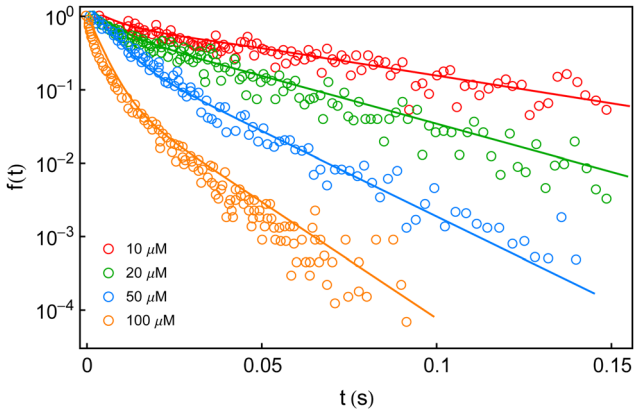

Fig. 3 Fall-offs of the waiting-time distributions of single β-galactosidase molecules measured at substrate concentrations of 10, 20, 50 and 100 μM (concentration increases downwards) in a log-linear scale (symbols).[7] The solid lines are the theoretical results (eqn (24)) deduced from the three-conformer dynamic-disorder model of single β-galactosidase catalysis (Fig. 2). The parameter values extracted from the fits are as follows: k_{b1} = 4.8 × 10^7 M^{-1} s^{-1}, k_{b2} = 9 × 10^7 M^{-1} s^{-1}, k_{b3} = 3 × 10^7 M^{-1} s^{-1}, k_{d1} = 18 300 s^{-1}, k_{d2} = 20 800 s^{-1}, k_{d3} = 12 300 s^{-1}, k_{c1} = 1050 s^{-1}, k_{c2} = 800 s^{-1}, and k_{c3} = 100 s^{-1}. λ_{ij}, λ_{ji}, ε_{ij} and ε_{ji} values were adjusted between 10 and 50 s^{-1} for best results. The choice of the fit parameters suggests the prevalence of dynamic disorder in the reaction pathway. The coefficient of determination for each plot was calculated as 0.99.

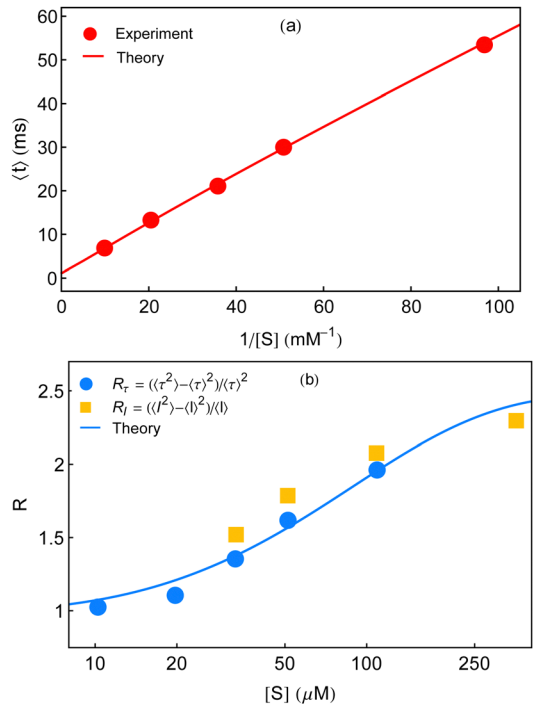

Fig. 4 Concentration dependence of the mean waiting time data (circles) and randomness parameter data (circles and squares) adopted from ref. 7. (a) The solid line is given by eqn (25). (b) The non-linear variation of R is explained from its definition using eqn (25) and (26). In both the plots, the magnitudes of the adjustable parameters, opted in Fig. 3, are kept the same.

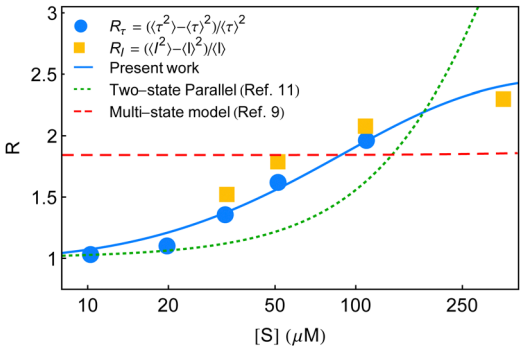

Fig. 5 Estimates of the randomness parameter calculated based on the two-state parallel model[11] (green dotted line) and the multi-state model[9] (red dashed line) are compared with the present result (blue solid line). Symbols represent the experimental data adopted from ref. 7.

The particulars of the two-state parallel and off-pathway models of single-enzyme catalytic turnover were assessed thoroughly in relation to the yields of the real time data.[11] The off-pathway mechanism designated a single route of product formation. However, fluctuations between the paired conformational isomers of E and ES were explicit in both the cases. The respective outputs were very close among which the lower magnitudes of the randomness parameter towards higher [S] were quite obvious. The partial quantitative agreement looked more similar to the exponential type of growth than the expected sigmoidal type increment. It was then opined that to elevate the mere qualitative estimates more counts of the conformational substates over the duplet are required. Noting the insensitivity of the multi-state kinetic formalism[9] towards the randomness data, we proposed a distinct model of dynamic disorder furnished with dynamic probes.[11] This model appeared superior to the two-state kinetic narration in delineating the multi-state structural heterogeneity supported by the reproducibility of the entire kinetic outputs. A mere adjustment of a single parameter, after some dimensional analysis, looked effective to describe the effect of substrate concentration besides utilizing a fairly smaller number of fit parameters. Although, as a substantial model it is valued, the reappraisal of the state-based kinetic treatment in this regard was wanting and in the present study, we, therefore, focused on this aspect. In Fig. 5, we summarize the comparisons of the randomness parameter data against the estimates of R calculated based on the two-state parallel model,[11] the present work and the multi-state model.[9]

A qualitative exploration to quantitative comparison of the single-enzyme kinetics were formalized by the conditions under which the suitability of MM equation holds good even in the circumstance of dynamic disorder.[7,9] An initial two-state model was generalized to accompany the rather realistic multi-state persuation of the fluctuating enzyme. Keen emphasis on the slower rates of conformational transition compared to the catalytic rate eventually resulted in a statically heterogeneous kinetic model. The waiting-time distribution was expressed in terms of the sum of the distributions of the individual waiting times related to every reaction channel multiplied by the allied steady-state weights. The latter are the ratios of the catalytic efficiencies of the distinct conformers to the sum of the catalytic efficiencies of all the individual conformers. To make the theoretical result competent in order to find comparison with the data, further assumptions like identical forward and backward rate constants and a continuum approximation were implemented. Consequently, the steady-state weights of each reaction channel appeared to vary with the catalytic rate constant. Ultimately, to reveal the different catalytic activities of the large number of ES species, the final assumption that the weight function suits a γ-distribution was invoked. As previously mentioned, the multi-state kinetic model remained ineffectual to respond to the variation of R as a function of [S] and thus cannot be recognised as foolproof. Hence, it seemed all-important to afresh the kinetic treatment fortified with a revised framework larger than the two-conformer model. This representation will envisage an explicit subsistence of the transition coefficients within the calculated results.

To elaborate the last point further, we employ the expression for $f(t)$ from eqn (24) of ref. 9 that is applicable for a three-state model, given by

$$f(t) = \sum_{i=1}^{3} w_i \frac{k_{1i}k_{2i}[\mathrm{S}]}{2A_i}[\exp(A_i + B_i)t - \exp(B_i - A_i)t] \qquad (27)$$

A_i and B_i are detailed just after the same equation. k_{1i}, k_{-1i} and k_{2i} are the rate constants for the steps of binding the substrate with i-th conformer of the enzyme, unbinding of the ES_i complex and the product formation from the ES_i complex, respectively. Here, the purpose of limiting the number of conformers to triplet is meant to additionally find comparison with our three-state description. We determined the individual weight factors w_i, shown below.

$$\begin{aligned}
w_1 &= \frac{k_{11}k_{21}(k_{-12}+k_{22})(k_{-13}+k_{23})}{k_{11}k_{21}(k_{-12}+k_{22})(k_{-13}+k_{23}) + (k_{-11}+k_{21})(k_{12}k_{22}(k_{-13}+k_{23}) + k_{13}k_{23}(k_{-12}+k_{22}))} \\
w_2 &= \frac{k_{12}k_{22}(k_{-11}+k_{21})(k_{-13}+k_{23})}{k_{11}k_{21}(k_{-12}+k_{22})(k_{-13}+k_{23}) + (k_{-11}+k_{21})(k_{12}k_{22}(k_{-13}+k_{23}) + k_{13}k_{23}(k_{-12}+k_{22}))} \\
w_3 &= \frac{k_{13}k_{23}(k_{-11}+k_{21})(k_{-12}+k_{22})}{k_{11}k_{21}(k_{-12}+k_{22})(k_{-13}+k_{23}) + (k_{-11}+k_{21})(k_{12}k_{22}(k_{-13}+k_{23}) + k_{13}k_{23}(k_{-12}+k_{22}))}
\end{aligned} \qquad (28)$$

In deriving eqn (28), the following relationship between w_i and the catalytic rate constants k_{2i} and the Michaelis constants K_{Mi} from ref. 9 are used

$$w_i = \frac{k_{Ei}}{\sum_{i=1}^{N} k_{Ei}} \tag{29}$$

where $k_{Ei} = k_{2i}/K_{Mi} = k_{2i}k_{1i}/(k_{-1i} + k_{2i})$. Now, having three isomers of the active species E and ES each, the conception that the different magnitudes of k_2 conform to a specific distribution would not be very meaningful. At the same time, even it lacks the rationality in governing the equilibrium reactions by the single rate constants either (two major assumptions of the multi-state model). Accordingly, assigning k_{1i}, k_{-1i}, k_{2i} as free fit parameters, we attempted to recover the experimental results and obtained good agreement for the case of the time-dependent decay of the histograms and the variation of the mean waiting times (figures not shown). On the other hand, the alternation of R with [S] (blue line) again ends up with the near constancy behaviour within the experimental range of substrate concentration, as previously demonstrated by the multi-state approach (red dashed line), shown in Fig. 6a. Evidently, in comparison to the theoretical prediction by our three-state model, we ascertain that certain presence of the transition rate coefficients within the calculated results seems paramount to follow the rise in the randomness parameter upon increasing the substrate concentration.

In view of the above result, the limiting conditions that restrained the form of the Michaelis–Menten equation[9] such as much greater catalytic rates relative to the interconversion rates of ES_i complexes, extremely slow structural transitions between the different ES conformers and extremely slow passage of one E conformer to another become incompetent in analysing the measurements of R presented in ref. 7. Moreover, the qualitative track of the randomness parameter shown in Fig. 6 of ref. 9 is quite different within the experimental range of substrate concentration to bring out the histograms of the waiting times. Note that, in producing Fig. 3 and 6a of the present work, the extracted values of the catalytic rate constants are similar. Importantly, the useful quantities of the parameters (λ and ε terms in Fig. 3) that are particularly relevant to the structural transitions are not limitingly small numbers and hence cannot be neglected. Our selection of the parameters thus aptly articulates the essence of dynamic disorder that involves changes in the conformations with rates comparable to or slower than the rates of chemical conversions.

As discussed in ref. 10, the expression for the multi-state waiting-time distribution, eqn (31) in Kou *et al.*'s work,[9] is characteristic for an ensemble of enzymes which possess the same rate constants of k_1 and k_{-1}, whereas the catalytic rate constants are all different. In turn, the same equation verily represents the average of the waiting-time distribution of the individual enzymes with a given probability density of the k_2 values. The inefficacy of the averaged distribution to expound the randomness quantified by R utterly reinforces the merit of the dynamic heterogeneity over the statically heterogeneous framework.

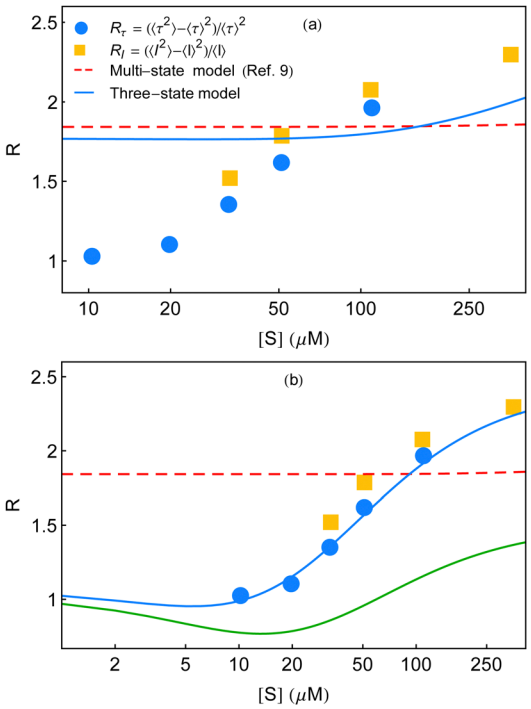

Fig. 6 Randomness parameter data (symbols) at different substrate concentrations[7] are compared with the theoretical expressions. (a) Multi-state model used in ref. 7 to compare the experimental results yields a constant estimate throughout (red dashed line) employing eqn (31) of ref. 9. The corresponding three-state model shows little growth at a much higher substrate concentration regime (blue line). The fit parameters, we used for the latter case, are as follows. $k_{11} = 5 \times 10^7$ M^{-1} s^{-1}, $k_{12} = 3 \times 10^7$ M^{-1} s^{-1}, $k_{13} = 6 \times 10^7$ M^{-1} s^{-1}, $k_{-11} = 18\,300$ s^{-1}, $k_{-12} = 21\,000$ s^{-1}, $k_{-13} = 11\,300$ s^{-1}, $k_{21} = 1150$ s^{-1}, $k_{22} = 800$ s^{-1}, and $k_{23} = 190$ s^{-1}. (b) Qualitative and quantitative explanations of the randomness parameter data adopted from English *et al.*[7] The red dashed line is identical with that in (a). The solid line that appears below the data (green line) is the qualitative plot of R (k_2 fluctuations) shown in Fig. 6 of ref. 9. We construct the quantitative comparison with the data (symbols), blue curve, with the aid of the multi-state formalism by Kou *et al.*[9] using the following set of fit parameters. $k_1 = 3.5 \times 10^7$ M^{-1} s^{-1}, $k_{-1} = 150$ s^{-1}, $a = 3.4$, and $b = 220$. The data set of waiting-time distributions and the mean waiting times cannot be regenerated utilizing these parameter values.

Jung *et al.* inquired that the randomness parameter (symbolized as Q and related to our notation of R by $Q = R - 1$) on account of a renewal reaction process disappears in the limit of low-substrate concentration. This is relevant to an ergodic and homogeneous reaction system and the reported enzymatic catalysis falls under the same grouping.[25] Again, it was verified in Yang *et al.*'s work[10] that the expression for the randomness parameter Q_{GC}, based on the generalized conventional chemical kinetics, does not meet the criteria for expected vanishing in the low substrate concentration limit onto any selection of the probability density function with a finite variance. Hence, the given definition of $f(t)$ in Kou *et al.*'s work was reviewed as inept to narrate the correct turnover-time distribution of the β-galactosidase enzyme. Nonetheless, we surveyed a distinct set of fit parameters for the multi-state

model that recovered the randomness parameter data in a quantitative manner. The corresponding result is displayed by the blue curve in Fig. 6b. The red line denotes the same estimate of R by the multi-state theory shown in Fig. 6a. The green curve represents the qualitative plot with k_2 fluctuations considered in ref. 9.

The unforeseen agreement observed here does not refute our inference based on the analysis made for Fig. 6a, discussed as follows. It is basic to match the histograms with the theory before checking conformity of the randomness parameter. Albeit, because of the isolated restoration of the randomness parameter data, we aspired to obtain a comparison with the remaining experimental outputs and acquired highly non-exponential decay profiles of the waiting-time distributions at 10 and 20 μM (figures not shown). The extent of non-exponentiality increased at the other concentrations too, following substantive disagreement between the predicted results and the data for the histograms and the mean waiting times. Therefore, starting from either satisfying the waiting-time distribution data or the randomness parameter data, the other one, in consequence, cannot be elucidated. The fact of limited applicability of the multi-state depiction towards the single-enzyme trial clearly reveals its inadequate proficiency.

Looking back at the present model, some points need be highlighted regarding the appropriateness of the three-state kinetic representation. First, ordinarily, one may behold there occurs little difference when the two-conformer scheme is raised to the three-conformer one. Nevertheless, it initiates an important prospect that conformational isomers are entitled to make additional transitions other than $E_{z-1} \leftrightarrow E_z \leftrightarrow E_{z+1}$ sequential interconversions. Accordingly, for the threefold reaction scenario, the primary (two-conformer) $E_1 \leftrightarrow E_2$ shifts are supplemented by $E_2 \leftrightarrow E_3$ and $E_1 \leftrightarrow E_3$ transformations. The same is valid for the ES species. More transitions appear naturally in the enlarged kinetic frameworks. The choicest feature of the three-conformer model is thus insightful owing to, in one side, the incapacity of the two-conformer scheme, governed by exclusive paired fluctuations, to explain the higher estimates of R and, on the other side, the fact of exceeding difficulty in dealing with an enlarged scheme accompanied by quite a large number of fit parameters. Since the three-state model provides worth agreement with the data, in practice, one needs not to employ any higher-state kinetic model beyond it to illustrate the experimental observations.

Second, in Fig. 7, we compare the calculated result of R with that obtained from the dynamic analysis.[11] It is seen that both the dynamic approach and the present kinetic approach recovered similar yields, although, the former is unrelated to the conventional stepwise chemical conversions. Here, it is to be noted that different realizations of the fluctuating bottleneck and the instantaneous distance between the two locations across the polymer chain may not result in a few conformational states. The ingenious way of evaluating the waiting-time distribution stemmed from the mutual integral-differential relationship with the survival probability. The latter was a dimensionless quantity and concerned only for the probability

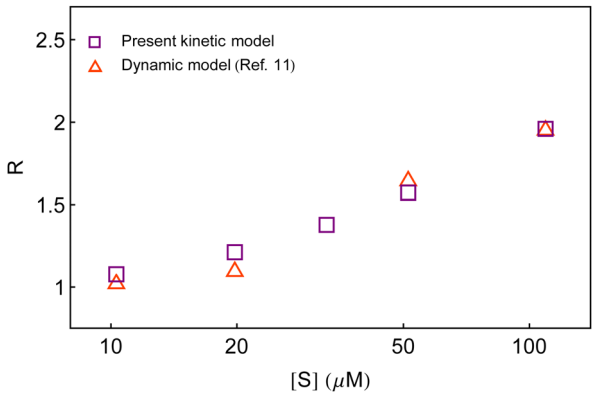

Fig. 7 Comparison of the estimates of the randomness parameter from the present kinetic model and the previous dynamic model.[11]

of the unreacted species (substrate) at a given time unconditioned to the detailed mechanism of product formation. Therefore, a dimensionally conditioned parameter was distinguished so as to exhibit the effect of substrate concentration. On the other hand, the state-based kinetic interpretation is subjected to the interest of individual active species undergoing transformation. The seeming difference between the two approaches, therefore, does not suggest to procure a one-to-one correspondence with regard to the number of conformational states. As a result, it is not surprising to conclude the closeness of the estimates of R produced by the three-conformer layout with that of the dynamic model. Nevertheless, we note that the kinetic model is preferred over the dynamic model to address the observables of single β-galactosidase catalysis because of its identity with the reaction mechanism, straightforward evaluation of the time-distribution function and the simplicity of direct variation of the substrate concentration.

The primary difference between the multi-state model of fluctuating enzyme by Kou *et al.*[9] and our threefold description is that the former has a large extent of conformational fluctuations which, in turn, were made generalized by the involved assumptions. The other one, however, possesses the opposite characteristics. In between these outlooks, there exist various kinetic frameworks with a different number of conformational states. Although, we justified for evading a finite-state model beyond the three-conformer case, it might be interesting to analyse whether a generalization can be made across the varying number of interconverting conformers (N = 2,3,4,. . .). In making progress from a lower kinetic scheme of N_1 conformers to higher N_2 conformers, the numbers of reaction paths and reaction rate constants increase by $N_2 - N_1$ and $3(N_2 - N_1)$, respectively, whereas the count of the conformational transitions increases by $2(N_2 - N_1)(N_2 + N_1 - 1)$. Once N is definite, the order of the matrix becomes fixed. This clearly means that the requisite calculations must be performed each time when any change is made in the count of N. The distinct expressions for $f(t)$ originated from the different schemes (different N) will be left unruled by a general structure owing to the forms of the denominators in the equations describing $P_{ES_i}(s)$ [degrees of the equations differ] and the coefficients η

and δ terms. Nevertheless, after scrutinizing the schemes with two, three and four parallel catalytic routes (N = 2, 3, 4), the following common appearances are realized which are valid for any finite N.

$$P_{\mathrm{ES}_1}(s) = \frac{\sum_{h=0}^{2N-2} \eta_{1h} s^h}{s^{2N} + \sum_{h=0}^{2N-1} \delta_h s^h} \tag{30}$$

$$P_{\mathrm{ES}_m}(s) = \frac{\sum_{h=0}^{2N-3} \eta_{mh} s^h}{s^{2N} + \sum_{h=0}^{2N-1} \delta_h s^h} \tag{31}$$

$$P_{\mathrm{ES}_1}(t) = \sum_{\theta=1}^{2N} \frac{(-1)^{h+1} \sum_{h=0}^{2N-2} \eta_{1h} r_\theta^h}{\prod_{\phi=1,\phi\neq\theta}^{2N} (r_\theta - r_\phi)} \mathrm{e}^{-r_\theta t} \tag{32}$$

$$P_{\mathrm{ES}_m}(t) = \sum_{\theta=1}^{2N} \frac{(-1)^{h+1} \sum_{h=0}^{2N-3} \eta_{mh} r_\theta^h}{\prod_{\phi=1,\phi\neq\theta}^{2N} (r_\theta - r_\phi)} \mathrm{e}^{-r_\theta t} \tag{33}$$

where m stands for the index of ES conformers ranging from 2 to N. η_{1h}, η_{mh} and δ_h are the combinatory rate parameters. r_θ and r_ϕ (θ and ϕ vary from 1 to 2N) are the effective rate constants, related to the roots of the equation $s^{2N} + \sum_{h=0}^{2N-1} \delta_h s^h = 0$. The histogram of the waiting times takes the form

$$\begin{aligned} f(t) &= k_{\mathrm{c1}} P_{\mathrm{ES}_1}(t) + \sum_{m=2}^{N} k_{\mathrm{c}m} P_{\mathrm{ES}_m}(t) \\ &= \sum_{\theta=1}^{2N} \frac{\mathrm{e}^{-r_\theta t}}{\prod_{\phi=1,\phi\neq\theta}^{2N} (r_\theta - r_\phi)} \Bigg[(-1)^{h+1} k_{\mathrm{c1}} \sum_{h=0}^{2N-2} \eta_{1h} r_\theta^h \\ &\quad + \sum_{m=2}^{N} (-1)^{h+1} k_{\mathrm{c}m} \sum_{h=0}^{2N-3} \eta_{mh} r_\theta^h \Bigg] \end{aligned} \tag{34}$$

Either eqn (24) (N = 3) or eqn (34) actualises the complex kinetics better than eqn (24) and (31) of ref. 9 since we did not invoke assumptions in our analysis. The three-conformer model was our first choice beyond a two-state description and we elicited the same to be minimal and indispensable to illustrate the findings of single-β-galactosidase catalysis fully.

4 Conclusion

Fluctuations in β-galactosidase catalysis were probed using the single-enzyme turnover experiments that analyzed the turnover time traces and restored the dynamic information by the observable waiting time distribution. In this work, we investigated using an analytical model the influence of dynamic disorder in the catalytic pathway, especially focusing on the distinctive relationship between the waiting time distribution data and the randomness parameter data. We established that a three-conformer model provided a minimal kinetic illustration of the single-enzymatic reaction that quantitatively reproduced the observed time variations of the waiting time distribution and the allied non-linear uprise of the randomness parameter from unity over the experimental range of substrate concentrations.

The added complexity of the current model in comparison to the elemental two-conformer dynamic disorder description became essential to minimally account for the flexibility in conformational transitions. This, however, appeared indispensable to elevate the calculated randomness at higher substrate concentrations. The direct application of our theoretical results to the single-β-galactosidase catalysis did not involve working assumptions as were associated with the previous multi-state analysis. The determination of the distribution function of the waiting times and its various moments must be accompanied by all the rate constants considered in the model. We showed that the view of retaining the transition coefficients is paramount since the expression for the waiting-time distribution unfurnished with those coefficients made the outcomes of the three-conformer layout indifferent to the randomness data. Besides satisfying the particularity of the connection between the waiting-time distribution data and the randomness parameter data, our results also led to successful recovery of the observed mean times for product formation. Our work thus suggests an effective stochastic kinetic theory where parallel transitions for the active conformers are acknowledged and the counts of the adjustable parameters are also least. The choice of the fit parameters remained worthy to discern the dynamic disorder scenario unlike the static heterogeneity prevailed in the multi-state formulation.

The interconnectivity of the kinetic schemes with the different numbers of conformational isomers is observed. Nevertheless, the structures of the waiting-time distribution for the case of N_1, N_2, N_3, ... conformational states cannot be made to obtain a generalized expression. Therefore, exercising with a higher-state kinetic framework beyond the three-state model to get back the similar agreement by means of more extensive calculations can be evaded.

Finally, we note that the conception of discrete state stochastic model and the mathematical strategy based on the Laplace transform employed here are also well applicable to other areas, such as DNA–protein binding kinetics[37] besides DNA escape kinetics,[21] force extension kinetics[22] and electron transfer kinetics.[24] The search of DNA-binding proteins for their specific target sites on DNA inside the living cell is an important biological phenomenon in regulating the cellular processes.[37,38] A target search on a straight DNA fragment[38] and the role of DNA loop formation and DNA conformational fluctuations[37] received rich theoretical investigations.

Conflicts of interest

There are no conflicts of interest to declare.

Appendices

Appendix A: structures of matrices in eqn (7)

The matrix $\mathbf{M}_{X_{\text{in}}}$ denotes the rates of the transitions from all X_js to any X_i. On the other hand, the matrix $\mathbf{M}_{X_{\text{out}}}$ denotes the rates of the transitions from any X_i to all X_js. These can be written as

$$\mathbf{M}_{X_{\text{in}}} = \begin{pmatrix} 0 & \lambda_{21} & \lambda_{31} & \cdots & \lambda_{N1} \\ \lambda_{12} & 0 & \lambda_{32} & \cdots & \lambda_{N2} \\ \lambda_{13} & \lambda_{23} & 0 & \cdots & \lambda_{N3} \\ \vdots & \vdots & \vdots & \ddots & \vdots \\ \lambda_{1N} & \lambda_{2N} & \lambda_{3N} & \cdots & 0 \end{pmatrix}$$

$$\mathbf{M}_{X_{\text{out}}} = \begin{pmatrix} \sum_{j=2}^{N} \lambda_{1j} & 0 & 0 & \cdots & 0 \\ 0 & \sum_{j=1,\, j\neq 2}^{N} \lambda_{2j} & 0 & \cdots & 0 \\ 0 & 0 & \sum_{j=1,\, j\neq 3}^{N} \lambda_{3j} & \cdots & 0 \\ \vdots & \vdots & \vdots & \ddots & \vdots \\ 0 & 0 & 0 & \cdots & \sum_{j=1}^{N-1} \lambda_{Nj} \end{pmatrix}$$

Similarly, matrices $\mathbf{M}_{Y_{\text{in}}}$ and $\mathbf{M}_{Y_{\text{out}}}$ representing the transition rates from all Y_js to any Y_i and *vice versa*, respectively are found to be

$$\mathbf{M}_{Y_{\text{in}}} = \begin{pmatrix} 0 & \varepsilon_{21} & \varepsilon_{31} & \cdots & \varepsilon_{N1} \\ \varepsilon_{12} & 0 & \varepsilon_{32} & \cdots & \varepsilon_{N2} \\ \varepsilon_{13} & \varepsilon_{23} & 0 & \cdots & \varepsilon_{N3} \\ \vdots & \vdots & \vdots & \ddots & \vdots \\ \varepsilon_{1N} & \varepsilon_{2N} & \varepsilon_{3N} & \cdots & 0 \end{pmatrix}$$

$$\mathbf{M}_{Y_{\text{out}}} = \begin{pmatrix} \sum_{j=2}^{N} \varepsilon_{1j} & 0 & 0 & \cdots & 0 \\ 0 & \sum_{j=1,\, j\neq 2}^{N} \varepsilon_{2j} & 0 & \cdots & 0 \\ 0 & 0 & \sum_{j=1,\, j\neq 3}^{N} \varepsilon_{3j} & \cdots & 0 \\ \vdots & \vdots & \vdots & \ddots & \vdots \\ 0 & 0 & 0 & \cdots & \sum_{j=1}^{N-1} \varepsilon_{Nj} \end{pmatrix}$$

Matrices $\mathbf{M}_{XY}$ and $\mathbf{M}_{YX}$ correspond to the transition rates from X_i's to Y_i's and the opposite way from Y_i's to X_i's. Finally, the matrix $\mathbf{M}_{YZ}$ indicates the conversion from Y_i's to the product. These are detailed as follows.

$$\mathbf{M}_{XY} = \begin{pmatrix} k_{\text{b1}}[\text{S}] & 0 & 0 & \cdots & 0 \\ 0 & k_{\text{b2}}[\text{S}] & 0 & \cdots & 0 \\ 0 & 0 & k_{\text{b3}}[\text{S}] & \cdots & 0 \\ \vdots & \vdots & \vdots & \ddots & \vdots \\ 0 & 0 & 0 & \cdots & k_{\text{b}N}[\text{S}] \end{pmatrix}$$

$$\mathbf{M}_{YX} = \begin{pmatrix} k_{\text{d1}} & 0 & 0 & \cdots & 0 \\ 0 & k_{\text{d2}} & 0 & \cdots & 0 \\ 0 & 0 & k_{\text{d3}} & \cdots & 0 \\ \vdots & \vdots & \vdots & \ddots & \vdots \\ 0 & 0 & 0 & \cdots & k_{\text{d}N} \end{pmatrix}$$

$$\mathbf{M}_{YZ} = \begin{pmatrix} k_{\text{c1}} & 0 & 0 & \cdots & 0 \\ 0 & k_{\text{c2}} & 0 & \cdots & 0 \\ 0 & 0 & k_{\text{c3}} & \cdots & 0 \\ \vdots & \vdots & \vdots & \ddots & \vdots \\ 0 & 0 & 0 & \cdots & k_{\text{c}N} \end{pmatrix}$$

Appendix B: exact expressions for the coefficients in eqn (17)–(19)

I. Coefficients in the numerators

$$\eta_{14} = k_{\text{b1}}[\text{S}]$$

$$\eta_{13} = k_{\text{b1}}[\text{S}](A_2 + B_2 + A_3 + B_3)$$

$$\begin{aligned}\eta_{12} = {} & k_{\text{b1}}[\text{S}](A_2(B_2 + A_3 + B_3) + A_3(B_2 + B_3) + B_2B_3) \\ & - k_{\text{b1}}[\text{S}](k_{\text{b2}}[\text{S}]k_{\text{d2}} + k_{\text{b3}}[\text{S}]k_{\text{d3}} + \varepsilon_{23}\varepsilon_{32} + \lambda_{23}\lambda_{32}) \\ & + k_{\text{b2}}[\text{S}]\varepsilon_{21}\lambda_{12} + k_{\text{b3}}[\text{S}]\varepsilon_{31}\lambda_{13}\end{aligned}$$

$$\begin{aligned}\eta_{11} = {} & k_{\text{b1}}[\text{S}]((A_2A_3 - \lambda_{23}\lambda_{32})(B_2 + B_3) + (B_2B_3 - \varepsilon_{23}\varepsilon_{32})(A_2 + A_3)) \\ & - k_{\text{b1}}[\text{S}](k_{\text{b2}}[\text{S}]k_{\text{d2}}(A_3 + B_3) + k_{\text{b3}}[\text{S}]k_{\text{d3}}(A_2 + B_2)) \\ & + k_{\text{b2}}[\text{S}](\varepsilon_{21}\lambda_{12}(A_3 + B_3) + \varepsilon_{23}\varepsilon_{31}\lambda_{12} + \varepsilon_{21}\lambda_{13}\lambda_{32}) \\ & + k_{\text{b3}}[\text{S}](\varepsilon_{31}\lambda_{13}(A_2 + B_2) + \varepsilon_{21}\varepsilon_{32}\lambda_{13} + \varepsilon_{31}\lambda_{12}\lambda_{23})\end{aligned}$$

$$\begin{aligned}\eta_{10} &= k_{b1}k_{b2}k_{b3}[S]^3k_{d2}k_{d3} - k_{b1}[S]^2(k_{b2}k_{d2}A_3B_3\\ &+ k_{b3}k_{d3}A_2B_2 + k_{b3}k_{d2}\varepsilon_{32}\lambda_{23} + k_{b2}k_{d3}\varepsilon_{23}\lambda_{32})\\ &- k_{b2}k_{b3}[S]^2(k_{d2}\varepsilon_{31}\lambda_{13} + k_{d3}\varepsilon_{21}\lambda_{12})\\ &+ k_{b1}[S](B_2B_3 - \varepsilon_{23}\varepsilon_{32})(A_2A_3 - \lambda_{23}\lambda_{32})\\ &+ k_{b2}[S](A_3\lambda_{12} + \lambda_{13}\lambda_{32})(B_3\varepsilon_{21} + \varepsilon_{23}\varepsilon_{31})\\ &+ k_{b3}[S](A_2\lambda_{13} + \lambda_{12}\lambda_{23})(B_2\varepsilon_{31} + \varepsilon_{21}\varepsilon_{32})\\ \eta_{23} &= (k_{b1}\varepsilon_{12} + k_{b2}\lambda_{12})[S]\\ \eta_{22} &= k_{b1}[S]\varepsilon_{12}(A_2 + A_3 + B_3) + k_{b1}[S]\varepsilon_{13}\varepsilon_{32}\\ &+ k_{b2}[S]\lambda_{12}(A_3 + B_1 + B_3) + k_{b2}[S]\lambda_{13}\lambda_{32} + k_{b3}[S]\varepsilon_{32}\lambda_{13}\\ \eta_{21} &= -k_{d3}[S]^2(k_{b1}k_{b3}\varepsilon_{12} + k_{b2}k_{b3}\lambda_{12})\\ &+ k_{b1}[S](\varepsilon_{12}(A_2A_3 + A_2B_3 + A_3B_3 - \lambda_{23}\lambda_{32})\\ &+ \varepsilon_{13}\varepsilon_{32}(A_2 + A_3))\\ &+ k_{b2}[S](\lambda_{12}(A_3B_1 + A_3B_3 + B_1B_3 - \varepsilon_{13}\varepsilon_{31})\\ &+ \lambda_{13}\lambda_{32}(B_1 + B_3))\\ &+ k_{b3}[S](\lambda_{13}(\varepsilon_{12}\varepsilon_{31} + A_2\varepsilon_{32} + B_1\varepsilon_{32}) + \lambda_{12}\lambda_{23}\varepsilon_{32})\\ \eta_{20} &= k_{d3}[S]^2(k_{b1}k_{b2}\varepsilon_{13}\lambda_{32} - A_2k_{b1}k_{b3}\varepsilon_{12} - B_1k_{b2}k_{b3}\lambda_{12})\\ &+ k_{b1}[S](A_2A_3 - \lambda_{23}\lambda_{32})(B_3\varepsilon_{12} + \varepsilon_{13}\varepsilon_{32})\\ &+ k_{b2}[S](B_1B_3 - \varepsilon_{13}\varepsilon_{31})(A_3\lambda_{12} + \lambda_{13}\lambda_{32})\\ &+ k_{b3}[S](A_2\lambda_{13} + \lambda_{12}\lambda_{23})(B_1\varepsilon_{32} + \varepsilon_{12}\varepsilon_{31})\\ \eta_{33} &= (k_{b1}\varepsilon_{13} + k_{b3}\lambda_{13})[S]\\ \eta_{32} &= k_{b1}[S]\varepsilon_{13}(A_2 + A_3 + B_2) + k_{b1}[S]\varepsilon_{12}\varepsilon_{23}\\ &+ k_{b2}[S]\varepsilon_{23}\lambda_{12} + k_{b3}[S]\lambda_{13}(A_2 + B_1 + B_2)\\ &+ k_{b3}[S]\lambda_{12}\lambda_{23}\\ \eta_{31} &= -k_{d2}[S]^2(k_{b1}k_{b2}\varepsilon_{13} + k_{b2}k_{b3}\lambda_{13})\\ &+ k_{b1}[S](\varepsilon_{13}(A_2A_3 + A_2B_2 + A_3B_2 - \lambda_{23}\lambda_{32})\\ &+ \varepsilon_{12}\varepsilon_{23}(A_2 + A_3))\\ &+ k_{b2}[S](\lambda_{12}(\varepsilon_{13}\varepsilon_{21} + A_3\varepsilon_{23} + B_1\varepsilon_{23}) + \lambda_{13}\lambda_{32}\varepsilon_{23})\\ &+ k_{b3}[S](\lambda_{13}(A_2B_1 + A_2B_2 + B_1B_2 - \varepsilon_{12}\varepsilon_{21})\\ &+ \lambda_{12}\lambda_{23}(B_1 + B_2))\\ \eta_{30} &= k_{d2}[S]^2(k_{b1}k_{b3}\varepsilon_{12}\lambda_{23} - A_3k_{b1}k_{b2}\varepsilon_{13} - B_1k_{b2}k_{b3}\lambda_{13})\\ &+ k_{b1}[S](A_2A_3 - \lambda_{23}\lambda_{32})(B_2\varepsilon_{13} + \varepsilon_{12}\varepsilon_{23})\\ &+ k_{b2}[S](A_3\lambda_{12} + \lambda_{13}\lambda_{32})(B_1\varepsilon_{23} + \varepsilon_{13}\varepsilon_{21})\\ &+ k_{b3}[S](B_1B_2 - \varepsilon_{12}\varepsilon_{21})(A_2\lambda_{13} + \lambda_{12}\lambda_{23})\end{aligned}$$

with $A_1 = k_{b1}[S] + \lambda_{12} + \lambda_{13}$, $A_2 = k_{b2}[S] + \lambda_{21} + \lambda_{23}$, $A_3 = k_{b3}[S] + \lambda_{31} + \lambda_{32}$ and $B_1 = k_{d1} + k_{c1} + \varepsilon_{12} + \varepsilon_{13}$, $B_2 = k_{d2} + k_{c2} + \varepsilon_{21} + \varepsilon_{23}$, $B_3 = k_{d3} + k_{c3} + \varepsilon_{31} + \varepsilon_{32}$.

II. Coefficients in the denominators

$$\begin{aligned}\delta_5 &= (A_1 + A_2 + A_3 + B_1 + B_2 + B_3)\\ \delta_4 &= A_1(A_2 + A_3 + B_1 + B_2 + B_3) + A_2(A_3 + B_1 + B_2 + B_3)\\ &+ A_3(B_1 + B_2 + B_3) + B_1(B_2 + B_3) + B_2B_3\\ &- (k_{b1}k_{d1} + k_{b2}k_{d2} + k_{b3}k_{d3})[S]\\ &- \varepsilon_{12}\varepsilon_{21} - \varepsilon_{13}\varepsilon_{31} - \varepsilon_{23}\varepsilon_{32} - \lambda_{12}\lambda_{21} - \lambda_{13}\lambda_{31} - \lambda_{23}\lambda_{32}.\end{aligned}$$

$$\begin{aligned}\delta_3 &= A_1(A_2+A_3)(B_1+B_2+B_3) + B_1(B_2+B_3)(A_1+A_2+A_3)\\ &+ A_2A_3(B_1+B_2+B_3+A_1) + B_2B_3(A_1+A_2+A_3+B_1)\\ &- k_{b1}[S]k_{d1}(A_2+A_3+B_2+B_3)\\ &- k_{b2}[S]k_{d2}(A_1+A_3+B_1+B_3)\\ &- k_{b3}[S]k_{d3}(A_1+A_2+B_1+B_2) - \varepsilon_{12}\varepsilon_{21}(A_1+A_2+A_3+B_3)\\ &- \varepsilon_{13}\varepsilon_{31}(A_1+A_2+A_3+B_2) - \varepsilon_{23}\varepsilon_{32}(A_1+A_2+A_3+B_1)\\ &- \lambda_{12}\lambda_{21}(A_3+B_1+B_2+B_3) - \lambda_{13}\lambda_{31}(A_2+B_1+B_2+B_3)\\ &- \lambda_{23}\lambda_{32}(A_1+B_1+B_2+B_3) - \varepsilon_{12}\varepsilon_{23}\varepsilon_{31} - \varepsilon_{13}\varepsilon_{21}\varepsilon_{32}\\ &- \lambda_{12}\lambda_{23}\lambda_{31} - \lambda_{13}\lambda_{21}\lambda_{32}\\ \delta_2 &= (B_2+B_3)(A_1A_2(A_3+B_1) + A_3B_1(A_1+A_2))\\ &+ (A_2+A_3)(A_1+B_1)B_2B_3 + A_2A_3B_2B_3\\ &+ A_1B_1(A_2A_3 + B_2B_3)\\ &+ [S]^2(k_{b1}k_{d1}(k_{b2}k_{d2} + k_{b3}k_{d3}) + k_{b2}k_{d2}k_{b3}k_{d3})\\ &- k_{b1}[S]k_{d1}(A_2(A_3+B_2+B_3) + A_3(B_2+B_3)\\ &+ B_2B_3 - \varepsilon_{23}\varepsilon_{32} - \lambda_{23}\lambda_{32})\\ &- k_{b2}[S]k_{d2}(A_3(A_1+B_1+B_3) + A_1(B_1+B_3)\\ &+ B_1B_3 - \varepsilon_{13}\varepsilon_{31} - \lambda_{13}\lambda_{31})\\ &- k_{b3}[S]k_{d3}(A_1(A_2+B_1+B_2) + A_2(B_1+B_2)\\ &+ B_1B_2 - \varepsilon_{12}\varepsilon_{21} - \lambda_{12}\lambda_{21})\\ &- \varepsilon_{12}\varepsilon_{21}(A_1(A_2+A_3+B_3) + A_2(A_3+B_3) + A_3B_3)\\ &- \varepsilon_{13}\varepsilon_{31}(A_1(A_2+A_3+B_2) + A_2(A_3+B_2) + A_3B_2)\\ &- \varepsilon_{23}\varepsilon_{32}(A_1(A_2+A_3+B_1) + B_1(A_2+A_3) + A_2A_3)\\ &- (\lambda_{12}\lambda_{21} + \lambda_{13}\lambda_{31} + \lambda_{23}\lambda_{32})(B_1(B_2+B_3) + B_2B_3\\ &- \varepsilon_{12}\varepsilon_{21} - \varepsilon_{13}\varepsilon_{31} - \varepsilon_{23}\varepsilon_{32})\\ &- (B_1+B_2+B_3)(A_3\lambda_{12}\lambda_{21} + A_2\lambda_{13}\lambda_{31} + A_1\lambda_{23}\lambda_{32}\\ &+ \lambda_{12}\lambda_{23}\lambda_{31} + \lambda_{13}\lambda_{21}\lambda_{32})\\ &- (A_1+A_2+A_3)(\varepsilon_{12}\varepsilon_{23}\varepsilon_{31} + \varepsilon_{13}\varepsilon_{21}\varepsilon_{32})\\ &- [S](k_{b1}k_{d2}\varepsilon_{12}\lambda_{21} + k_{b1}k_{d3}\varepsilon_{13}\lambda_{31} + k_{b2}k_{d1}\varepsilon_{21}\lambda_{12}\\ &+ k_{b2}k_{d3}\varepsilon_{23}\lambda_{32} + k_{b3}k_{d1}\varepsilon_{31}\lambda_{13} + k_{b3}k_{d2}\varepsilon_{32}\lambda_{23})\end{aligned}$$

$$\begin{aligned}\delta_1 = {} & A_1A_2A_3(B_1B_2+B_2B_3+B_3B_1)+B_1B_2B_3(A_1A_2+A_2A_3+A_3A_1)\\ & +[\mathrm{S}]^2((A_3+B_3)k_{b1}k_{b2}k_{d1}k_{d2}+(A_2+B_2)k_{b1}k_{b3}k_{d1}k_{d3}\\ & +(A_1+B_1)k_{b2}k_{b3}k_{d2}k_{d3})\\ & -k_{b1}[\mathrm{S}]k_{d1}((B_2+B_3)(A_2A_3-\lambda_{23}\lambda_{32})\\ & +(A_2+A_3)(B_2B_3-\varepsilon_{23}\varepsilon_{32}))\\ & -k_{b2}[\mathrm{S}]k_{d2}((B_1+B_3)(A_1A_3-\lambda_{13}\lambda_{31})\\ & +(A_1+A_3)(B_1B_3-\varepsilon_{13}\varepsilon_{31}))\\ & -k_{b3}[\mathrm{S}]k_{d3}((B_1+B_2)(A_1A_2-\lambda_{12}\lambda_{21})\\ & +(A_1+A_2)(B_1B_2-\varepsilon_{12}\varepsilon_{21}))\\ & -\varepsilon_{12}\varepsilon_{21}(A_1A_2(A_3+B_3)+A_3B_3(A_1+A_2)-(A_3+B_3)\lambda_{12}\lambda_{21}\\ & -(A_2+B_3)\lambda_{13}\lambda_{31}-(A_1+B_3)\lambda_{23}\lambda_{32})\\ & -\varepsilon_{13}\varepsilon_{31}(A_1A_3(A_2+B_2)+A_2B_2(A_1+A_3)-(A_3+B_2)\lambda_{12}\lambda_{21}\\ & -(A_2+B_2)\lambda_{13}\lambda_{31}-(A_1+B_2)\lambda_{23}\lambda_{32})\\ & -\varepsilon_{23}\varepsilon_{32}(A_2A_3(A_1+B_1)+A_1B_1(A_2+A_3)-(A_3+B_1)\lambda_{12}\lambda_{21}\\ & -(A_2+B_1)\lambda_{13}\lambda_{31}-(A_1+B_1)\lambda_{23}\lambda_{32})\\ & -(\varepsilon_{12}\varepsilon_{23}\varepsilon_{31}+\varepsilon_{32}\varepsilon_{21}\varepsilon_{13})\\ & (A_1A_2+A_1A_3+A_2A_3-\lambda_{12}\lambda_{21}-\lambda_{13}\lambda_{31}-\lambda_{23}\lambda_{32})\\ & -(\lambda_{12}\lambda_{23}\lambda_{31}+\lambda_{32}\lambda_{21}\lambda_{13})\\ & (B_1B_2+B_1B_3+B_2B_3-\varepsilon_{12}\varepsilon_{21}-\varepsilon_{13}\varepsilon_{31}-\varepsilon_{23}\varepsilon_{32})\\ & -\lambda_{12}\lambda_{21}(B_1B_2(A_3+B_3)+A_3B_3(B_1+B_2))\\ & -\lambda_{13}\lambda_{31}(B_2B_3(A_2+B_1)+A_2B_1(B_2+B_3))\\ & -\lambda_{23}\lambda_{32}(B_1B_3(A_1+B_2)+A_1B_2(B_1+B_3))\\ & -k_{b1}[\mathrm{S}]k_{d2}(\varepsilon_{12}\lambda_{21}(A_3+B_3)+\varepsilon_{13}\varepsilon_{32}\lambda_{21}+\varepsilon_{12}\lambda_{23}\lambda_{31})\\ & -k_{b1}[\mathrm{S}]k_{d3}(\varepsilon_{13}\lambda_{31}(A_2+B_2)+\varepsilon_{12}\varepsilon_{23}\lambda_{31}+\varepsilon_{13}\lambda_{21}\lambda_{32})\\ & -k_{b2}[\mathrm{S}]k_{d1}(\varepsilon_{21}\lambda_{12}(A_3+B_3)+\varepsilon_{23}\varepsilon_{31}\lambda_{12}+\varepsilon_{21}\lambda_{13}\lambda_{32})\\ & -k_{b2}[\mathrm{S}]k_{d3}(\varepsilon_{23}\lambda_{32}(A_1+B_1)+\varepsilon_{13}\varepsilon_{21}\lambda_{32}+\varepsilon_{23}\lambda_{12}\lambda_{31})\\ & -k_{b3}[\mathrm{S}]k_{d1}(\varepsilon_{31}\lambda_{13}(A_2+B_2)+\varepsilon_{21}\varepsilon_{32}\lambda_{13}+\varepsilon_{31}\lambda_{12}\lambda_{23})\\ & -k_{b3}[\mathrm{S}]k_{d2}(\varepsilon_{32}\lambda_{23}(A_1+B_1)+\varepsilon_{12}\varepsilon_{31}\lambda_{23}+\varepsilon_{32}\lambda_{13}\lambda_{21})\end{aligned}$$

$$\begin{aligned}\delta_0 = {} & -[\mathrm{S}]^3k_{b1}k_{b2}k_{b3}k_{d1}k_{d2}k_{d3}\\ & +[\mathrm{S}]^2(k_{b1}k_{d1}(k_{b2}k_{d2}A_3B_3+k_{b2}k_{d3}\varepsilon_{23}\lambda_{32}+k_{b3}k_{d3}A_2B_2\\ & +k_{b3}k_{d2}\varepsilon_{32}\lambda_{23})+k_{b2}k_{d2}(k_{b3}k_{d3}A_1B_1\\ & +k_{b3}k_{d1}\varepsilon_{31}\lambda_{13}+k_{b1}k_{d3}\varepsilon_{13}\lambda_{31})\\ & +k_{b3}k_{d3}(k_{b1}k_{d2}\varepsilon_{12}\lambda_{21}+k_{b2}k_{d1}\varepsilon_{21}\lambda_{12}))\\ & -k_{b1}[\mathrm{S}]k_{d1}(B_2B_3-\varepsilon_{23}\varepsilon_{32})(A_2A_3-\lambda_{23}\lambda_{32})\\ & -k_{b2}[\mathrm{S}]k_{d2}(B_1B_3-\varepsilon_{13}\varepsilon_{31})(A_1A_3-\lambda_{13}\lambda_{31})\\ & -k_{b3}[\mathrm{S}]k_{d3}(B_1B_2-\varepsilon_{12}\varepsilon_{21})(A_1A_2-\lambda_{12}\lambda_{21})\\ & -k_{b1}[\mathrm{S}]k_{d2}(B_3\varepsilon_{12}+\varepsilon_{13}\varepsilon_{32})(A_3\lambda_{21}+\lambda_{23}\lambda_{31})\\ & -k_{b1}[\mathrm{S}]k_{d3}(B_2\varepsilon_{13}+\varepsilon_{12}\varepsilon_{23})(A_2\lambda_{31}+\lambda_{21}\lambda_{32})\\ & -k_{b2}[\mathrm{S}]k_{d1}(B_3\varepsilon_{21}+\varepsilon_{23}\varepsilon_{31})(A_3\lambda_{12}+\lambda_{13}\lambda_{32})\\ & -k_{b2}[\mathrm{S}]k_{d3}(B_1\varepsilon_{23}+\varepsilon_{13}\varepsilon_{21})(A_1\lambda_{32}+\lambda_{12}\lambda_{31})\\ & -k_{b3}[0\mathrm{S}]k_{d1}(B_2\varepsilon_{31}+\varepsilon_{21}\varepsilon_{32})(A_2\lambda_{13}+\lambda_{12}\lambda_{23})\\ & -k_{b3}[\mathrm{S}]k_{d2}(B_1\varepsilon_{32}+\varepsilon_{12}\varepsilon_{31})(A_1\lambda_{23}+\lambda_{13}\lambda_{21})\\ & -(\varepsilon_{12}\varepsilon_{23}\varepsilon_{31}+\varepsilon_{13}\varepsilon_{21}\varepsilon_{32})\\ & \times(A_1A_2A_3-A_3\lambda_{12}\lambda_{21}-A_2\lambda_{13}\lambda_{31}-A_1\lambda_{23}\lambda_{32})\\ & -(\varepsilon_{12}\varepsilon_{23}\varepsilon_{31}+\varepsilon_{13}\varepsilon_{21}\varepsilon_{32})(-\lambda_{12}\lambda_{23}\lambda_{31}-\lambda_{13}\lambda_{21}\lambda_{32})\\ & -(\lambda_{12}\lambda_{23}\lambda_{31}+\lambda_{13}\lambda_{21}\lambda_{32})\\ & \times(B_1B_2B_3-B_1\varepsilon_{23}\varepsilon_{32}-B_2\varepsilon_{13}\varepsilon_{31}-B_3\varepsilon_{12}\varepsilon_{21})\\ & -(A_1\lambda_{23}\lambda_{32}+A_2\lambda_{13}\lambda_{31}+A_3\lambda_{12}\lambda_{21}-A_1A_2A_3)\\ & \times(B_1B_2B_3-B_1\varepsilon_{23}\varepsilon_{32}-B_2\varepsilon_{13}\varepsilon_{31}-B_3\varepsilon_{12}\varepsilon_{21})\end{aligned}$$

with A_1, A_2, A_3 and B_1, B_2, B_3 as defined before.

Acknowledgements

P. K. acknowledges the financial support from S. N. Bose National Centre for Basic Sciences, Government of India.

Notes and references

1 M. Michaelis and M. L. Menten, Die kinetik der invertinwirkung, *Biochem. Z.*, 1913, **49**, 333–369.
2 H. P. Lu, L. Xun and X. S. Xie, Single-Molecule enzymatic dynamics, *Science*, 1998, **282**, 1877–1882.
3 X. Zhuang, H. Kim, M. J. B. Pereira, H. P. Babcock, N. G. Walter and S. Chu, Correlating structural dynamics and function in single ribozyme molecules, *Science*, 2002, **296**, 1473–1476.
4 A. M. van Oijen, P. C. Blainey, D. J. Crampton, C. C. Richardson, T. Ellenberger and X. S. Xie, Single-molecule kinetics of λ-exonuclease reveal base dependence and dynamic disorder, *Science*, 2003, **301**, 1235–1238.
5 O. Flomenbom and K. Velonia, *et al.*, Stretched exponential decay and correlations in the catalytic activity of fluctuating single lipase molecules, *Proc. Natl. Acad. Sci. U. S. A.*, 2005, **102**, 2368–2372.
6 K. Velonia and O. Flomenbom, *et al.*, Single-enzyme kinetics of CALB-catalyzed hydrolysis, *Angew. Chem., Int. Ed.*, 2005, **44**, 560–564.
7 B. P. English, W. Min, A. M. van Oijen, K. T. Lee, G. Luo, H. Sun, B. J. Cherayil, S. C. Kou and X. S. Xie, Ever-fluctuating single enzyme molecules: Michaelis-Menten equation revisited, *Nat. Chem. Biol.*, 2006, **2**, 87–94.

8 P. Atkins and J. de Paula, *Physical Chemistry*, Oxford University Press, U. K., 2006.
9 S. C. Kou, B. J. Cherayil, W. Min, B. P. English and X. S. Xie, Single-molecule Michaelis-Menten equations, *J. Phys. Chem. B*, 2005, **109**, 19068–19081.
10 S. Yang, J. Cao, R. J. Silbey and J. Sung, Quantitative interpretation of the randomness in single enzyme turnover times, *Biophys. J.*, 2011, **101**, 519–524.
11 P. Kundu, S. Saha and G. Gangopadhyay, A revisit to turnover kinetics of individual *Escherichia coli* β-galactosidase molecules, *J. Phys. Chem. B*, 2021, **125**, 8010–8020.
12 A. Kumar, H. Maity and A. Dua, Parallel versus off-pathway Michaelis-Menten mechanism for single-enzyme kinetics of a fluctuating enzyme, *J. Phys. Chem. B*, 2015, **119**, 8490–8500.
13 M. Wanunu, B. Chakrabarti, J. Mathe, D. R. Nelson and A. Meller, Orientation-dependent interactions of DNA with an α -hemolysin channel, *Phys. Rev. E: Stat., Nonlinear, Soft Matter Phys.*, 2008, **77**, 031904.
14 T. L. Kuo and S. Garcia-Manyes, *et al.*, Probing static disorder in Arrhenius kinetics by single-molecule force spectroscopy, *Proc. Natl. Acad. Sci. U. S. A.*, 2010, **107**, 11336–11340.
15 M. Schlierf, H. Li and J. M. Fernandez, The unfolding kinetics of ubiquitin captured with single-molecule force-clamp techniques, *Proc. Natl. Acad. Sci. U. S. A.*, 2004, **101**, 7299–7304.
16 A. F. Oberhauser, P. K. Hansma, M. Carrion-Vazquez and J. M. Fernandez, Stepwise unfolding of titin under force-clamp atomic force microscopy, *Proc. Natl. Acad. Sci. U. S. A.*, 2000, **98**, 468–472.
17 M. Schlierf and M. Rief, Single-molecule unfolding force distributions reveal a funnel-shaped energy landscape, *Biophys. J.*, 2006, **90**, L33–L35.
18 T. Strunz, K. Oroszlan, R. Schafer and H. J. Güntherodt, Dynamic force spectroscopy of single DNA molecules, *Proc. Natl. Acad. Sci. U. S. A.*, 1999, **96**, 11277–11282.
19 H. M. Piwonski, M. Goomanovsky, D. Bensimon, A. Horovitz and G. Haran, Allosteric inhibition of individual enzyme molecules trapped in lipid vesicles, *Proc. Natl. Acad. Sci. U. S. A.*, 2012, **109**, E1437–E1443.
20 H. Wang, S. Lin, J. P. Allen, J. C. Williams, S. Blankert, C. Laser and N. W. Woodbury, Protein dynamics control the kinetics of initial electron transfer in photosynthesis, *Science*, 2007, **316**, 747–750.
21 P. Kundu, S. Saha and G. Gangopadhyay, Stochastic kinetic approach to the escape of DNA hairpins from an α -hemolysin channel, *J. Phys. Chem. B*, 2020, **124**, 6575–6584.
22 P. Kundu, S. Saha and G. Gangopadhyay, An exactly solvable stochastic kinetic theory of single-molecule force experiments, *J. Phys. Chem. B*, 2020, **124**, 7735–7744.
23 P. Kundu, S. Saha and G. Gangopadhyay, Kinetics of allosteric inhibition of single enzyme by product molecules, *J. Phys. Chem. B*, 2020, **124**, 11793–11801.
24 P. Kundu, Kinetics of initial charge separation in the photosynthetic reaction centers of *Rhodobacter sphaeroides*, *J. Phys. Chem. B*, 2022, **126**, 3470–3476.
25 W. Jung, S. Yang and J. Sung, Novel chemical kinetics for a single enzyme reaction: relationship between substrate concentration and the second moment of enzyme reaction time, *J. Phys. Chem. B*, 2010, **114**, 9840–9847.
26 R. Zwanzig, Dynamical disorder: passage through a fluctuating bottleneck, *J. Chem. Phys.*, 1992, **97**, 3587–3589.
27 M. Doi and S. F. Edwards, *The Theory of Polymer Dynamics*, Clarendon, Oxford, 1986.
28 A. Y. Grosberg and A. R. Khokhlov, *Statistical Physics of Macromolecules*, American Institute of Physics, New York, 1994.
29 C. W. Gardiner, *Handbook of Stochastic Methods for Physics, Chemistry and Natural Sciences*, Springer-Verlag, Berlin, Germany, 2004.
30 N. G. Van Kampen, *Stochastic Processes in Physics and Chemistry*, Elsevier, New York, 2007.
31 D. A. McQuarrie, Stochastic approach to chemical kinetics, *J. Appl. Probab.*, 1967, **4**, 413–478.
32 S. Saha, A. Sinha and A. Dua, Single-molecule enzyme kinetics in the presence of inhibitors, *J. Chem. Phys.*, 2012, **137**, 045102.
33 J. L. Schiff, *The Laplace Transform: Theory and Applications*, Springer-Verlag, New York, 1999.
34 S. Render, *A Guide to First-passage Processes*, Cambridge University Press, New York, 2001.
35 P. Lecca, I. Laurenzi and F. Jordan, *Deterministic versus Stochastic Modelling in Biochemistry and Systems Biology*, Woodhead Publishing, U.S.A., 2013.
36 J. R. Moffitt and C. Bustamante, Extracting signal from noise: kinetic mechanisms from a Michaelis-Menten-like expression for enzymatic fluctuations, *FEBS J.*, 2014, **281**, 498–517.
37 C. Felipe, J. Shin and A. B. Kolomeisky, DNA looping and DNA conformational fluctuations can accelerate protein target search, *J. Phys. Chem. B*, 2021, **125**, 1727–1734.
38 P. Kar, A. G. Cherstvy and R. Metzler, Acceleration of bursty multiprotein target search kinetics on DNA by colocalisation, *Phys. Chem. Chem. Phys.*, 2018, **20**, 7931–7946.

